Biophysical Journal, Volume *111*

Supplemental Information

^{2}H-NMR and MD Simulations Reveal Membrane-Bound Conformation of Magainin 2 and Its Synergy with PGLa

Erik Strandberg, Diana Horn, Sabine Reißer, Jonathan Zerweck, Parvesh Wadhwani, and Anne S. Ulrich

Biophysical Journal, Volume *111*
Supporting Material

^{2}H-NMR and MD Simulations Reveal Membrane-Bound Conformation of Magainin 2 and Its Synergy with PGLa

Erik Strandberg,[1] Diana Horn,[2] Sabine Reißer,[1,3] Jonathan Zerweck,[2] Parvesh Wadhwani,[1] Anne S. Ulrich[1,2,*]

[1] Institute of Biological Interfaces (IBG-2), [2] Institute of Organic Chemistry, and [3] Institute of Physical Chemistry, Karlsruhe Institute of Technology, Karlsruhe, Germany;

* Corresponding author. Email: anne.ulrich@kit.edu

MATERIALS AND METHODS

Materials

All Fmoc protected amino acids where purchased from Iris Biotech GmbH (Marktredwitz, Germany) or Novabiochem (Merck Chemicals Ltd, Nottingham, UK), except for 3,3,3-$^2H_3$-*L*-alanine (Ala-d_3), which was purchased from Cambridge Isotope Laboratories (Andover, USA). Deuterium-depleted water was from Acros Organics (Geel, Belgium), and other solvents were from Acros Organics, Merck (Darmstadt, Germany), Fisher Scientific (Schwerte, Germany), or Biosolve (Valkenswaard, The Netherlands). The lipids 1,2-dimyristoyl-*sn*-glycero-3-phosphatidylcholine (DMPC), 1,2-dimyristoyl-*sn*-glycero-3-phosphatidylglycerol (DMPG), 1-palmitoyl-2-oleoyl-*sn*-glycero-3-phosphatidylcholine (POPC), and 1-palmitoyl-2-oleoyl-*sn*-glycero-3-phosphatidylglycerol (POPG) were purchased from Avanti Polar Lipids (Alabaster, AL, USA).

Peptide synthesis

Ala-d_3 was incorporated at specific positions in magainin 2 (MAG2) with the amino acid sequence GIGKFLHSAKKFGKAFVGEIMNS (**Table S1**). For peptide synthesis, standard Fmoc solid phase protocols were used (1), as previously described in detail (2).

Table S1. Synthesized peptides used in this study.

Peptide	**Substituted position**	**Sequence**
MAG2-WT	-	GIGKFLHSAKKFGKAFVGEIMNS
MAG2-F5A	Phe-5	GIGK-**Ala-d_3**-LHSAKKFGKAFVGEIMNS
MAG2-L6A	Leu-6	GIGKF-**Ala-d_3**-HSAKKFGKAFVGEIMNS
MAG2-A9	Ala-9	GIGKFLHS-**Ala-d_3**-KKFGKAFVGEIMNS
MAG2-F12A	Phe-12	GIGKFLHSAKK-**Ala-d_3**-GKAFVGEIMNS
MAG2-G13A	Gly-13	GIGKFLHSAKKF-**Ala-d_3**-KAFVGEIMNS
MAG2-A15	Ala-15	GIGKFLHSAKKFGK-**Ala-d_3**-FVGEIMNS
MAG2-F16A	Phe-16	GIGKFLHSAKKFGKA-**Ala-d_3**-VGEIMNS
MAG2-V17A	Val-17	GIGKFLHSAKKFGKAF-**Ala-d_3**-GEIMNS
MAG2-G18A	Gly-18	GIGKFLHSAKKFGKAFV-**Ala-d_3**-EIMNS
MAG2-I20A	Ile-20	GIGKFLHSAKKFGKAFVGE-**Ala-d_3**-MNS
PGLa	-	GMASKAGAIAGKIAKVALKAL-NH_2

Solid-state NMR

NMR sample preparation. Usually 0.5-1 mg of ^{2}H-labeled peptide was used in each sample, together with appropriate amounts of lipids to obtain the desired P/L ratio. In samples including PGLa, around 0.5 mg of the ^{2}H-labeled MAG2 analog and an equimolar amount of unlabeled PGLa was used. In short, oriented NMR samples were prepared by co-dissolving the lipid and peptide, spreading the mixture on 9 mm × 7.5 mm × 0.08 mm glass plates (Marienfeld, Lauda-Königshofen, Germany), drying to remove the solvent, and subsequent hydration at 48°C in 96% relative humidity using a saturated solution of K_2SO_4 in deuterium-depleted water (DDW) for 16-20 h. Due to problems with peptide aggregation and getting well-resolved NMR splittings at high P/L, several different methods were tried. In the *standard method* (method 1), which worked well in POPC/POPC and at P/L=1:100, the lipids were dissolved separately in 200 µl

$CHCl_3$/MeOH (1/1 v/v) and mixed in one vessel with vortexing and sonication. Peptides were dissolved in 100 µl MeOH and then mixed into the lipid solution. In some cases, when the solution was not clear, 20 µl DDW was added, and the solution was vortexed and sonicated. This solution was then spread on glass plates. In the *MLV method* (method 2), a peptide-lipid solution was prepared as in the standard method. This solution was dried under argon gas to a film and then dried further in vacuum for 1 h. The dry film was hydrated with 105 µl DDW, mixed, centrifuged, and freeze-thawed five times, to get a homogeneous, milk-like suspension. This suspension was spread onto the glass plates, which were dried in air >1 h and then under vacuum for 22 h to remove all water completely before hydration. In the *two-step method* (method 3), the peptides were first dissolved in MeOH, and after vortexing and sonification the peptide solution was spread on glass plates and air-dried. Then the lipids were dissolved in $CHCl_3$/MeOH, and after vortexing and sonication the lipid solution was spread on the glass plates on top of the peptide film. After air-drying the plates were dried under vacuum for 22 h before hydration.

Experimental parameters. Solid-state NMR experiments were carried out on 500 MHz and 600 MHz Bruker Avance NMR spectrometers (Bruker Biospin, Karlsruhe, Germany). ^{31}P-NMR was performed using a Hahn-echo sequence with ^{1}H decoupling (3), and ^{2}H-NMR was performed with a solid-echo sequence (4). Typical 90º pulse lengths were 4-5 µs. Further NMR experimental details have been published previously (5). The oriented samples were measured with the bilayer normal parallel to the external magnetic field.

NMR data analysis. The orientation of a helical peptide in the membrane can be described by two angles: the tilt angle τ, defined as the angle between the long axis of the helix and the membrane normal, and the azimuthal rotation angle ρ, which defines the rotation of the peptide around its long axis (see **Figure S1**). Using ^{2}H-NMR data from Ala-d_3 labeled positions, the helix orientation is calculated from RMSD fits and quadrupolar wave plots, as described previously (6-8).

To calculate orientational constraints from the NMR data, a quadrupolar coupling constant (e^2qQ/h) of 167 kHz for an aliphatic C-D bond was used, giving a maximum quadrupole splitting of 84 kHz for the CD_3-groups of the Ala-d_3 labels (9). The quadrupole splitting $\Delta\nu_q$ is then given by

$$\Delta\nu_q = 84 \text{ kHz} \times \tfrac{1}{2}\langle 3\cos^2\theta - 1\rangle \qquad (1)$$

where ⟨ ⟩ represents the time average, and θ is the angle between the C-CD_3 bond and the external magnetic field B_0.

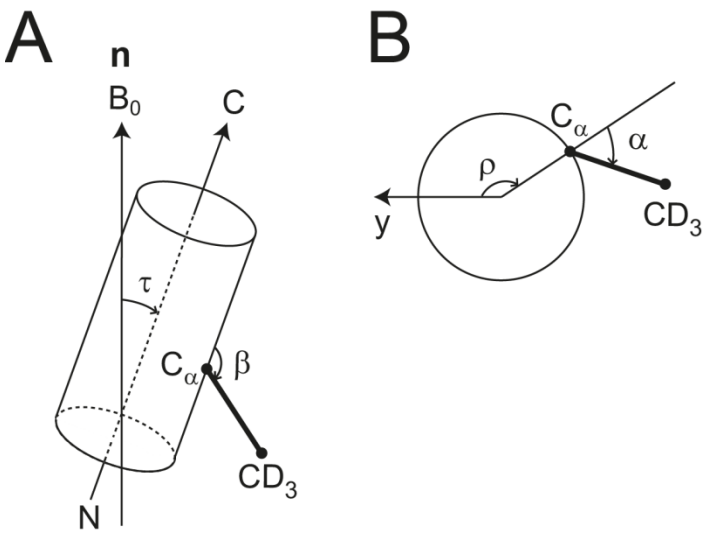

Figure S1. Definition of angles used in this work. (A) The helix tilt angle τ is the angle between the peptide axis (from N- to C-terminus) and the bilayer normal **n** (which in NMR experiments is usually aligned parallel to the magnetic field direction B_0). For τ = 0°, the helix would be oriented along **n**. The angle β fixes the C_α-CD_3 bond vector relative to the helix axis. (B) View perpendicular to the helix axis, with the C-terminus pointing out of the paper plane. The azimuthal rotation of the peptide is defined by the angle ρ. We define ρ = 0° such that the radial vector from the helix center through the C_α atom of residue 12 is aligned with the y-axis, which is parallel to the membrane surface. The projection of the C_α-CD_3 bond vector onto the plane perpendicular to the helix axis is fixed by the angle α.

For the NMR analysis, the structure of MAG2 was modeled as an ideal α-helix, and the alignment of this helix was fitted to the orientational constraints. In the molecular frame, the tilt angle τ defines the angle between the helix axis (defined from the N- to the C-terminus) and the bilayer normal. The azimuthal angle ρ is defined as a right-handed rotation around the helix axis, where ρ = 0° means that a radial vector from the helix axis to the C_α-atom of Phe-12 is oriented parallel to the membrane surface (6,10). The orientation of the C_α-C_β bond in the molecular frame is described by an angle β between the bond vector and the helix axis, and an angle α, defined by the vector radiating from the helix axis through the C_α-atom and by the projection of the C_α-C_β bond vector onto a plane perpendicular to the helix. In the same plane, the rotational angle between two consecutive amino acids along the helix is called ω. The angles are explained

in **Figure S1**. We described an α-helix using a β of 121.1°, an α of 53.2°, and an ω of 100°, as determined from an α-helical polyalanine model constructed in SYBYL (Tripos, St. Louis, USA) using the torsion angles φ = -58° and ψ = -47° (10).

Peptide dynamics are described in terms of whole-body fluctuations by Gaussian distributions of the τ and ρ angles, with widths given by the standard deviations σ_τ and σ_ρ, respectively. Larger widths correspond to a more dynamic situation, in which the angles undergo more vigorous fluctuations with larger amplitudes. It is justified to assume that these fluctuations are fast on the NMR time scale, so that the measured splittings represent time-averages over these distributions (11,12). In a grid search for the best-fit peptide structure, the helix is systematically rotated, and the theoretical quadrupole splittings are calculated for different combinations of τ, ρ, σ_τ and σ_ρ. All parameters are changed in steps of 1°; τ and ρ are investigated over the range from 0 to 180°, and σ_τ and σ_ρ from 0 to 50°, which was found to be a large enough range of dynamics to cover the point with the lowest root-mean-square deviation (RMSD) with respect to the experimental data. This way, we identified the best-fit parameters τ, ρ, σ_τ and $\sigma_{\rho,}$ which describe the orientation and dynamics of the peptide.

Molecular dynamics simulations

Simulation setup and parameters. Simulations were conducted for a single MAG2 in a DMPC bilayer consisting of 128 lipids solvated with 5700 TIP3P water molecules (13) and neutralized with chloride ions, and in a DMPC/DMPG bilayer with 96 DMPC and 32 DMPG lipids with 7000 water molecules and neutralized with sodium ions. The SLIPID force field was used for the lipids (14), and the AMBER99SB-ILDN (15) force field for everything else. This parameter combination has been used earlier, where it was shown that experimental parameters are well reproduced (16). The peptides were initially modeled as ideal α-helices using the *xleap* tool from the AmberTools modeling suite, using backbone torsion angles of φ = -57° and ψ= -47° (17). Simulations were performed with the GROMACS simulation package version 4.5.5 (simulation in DMPC) and 4.6.3 (simulation in DMPC/DMPG). The peptide-membrane complexes were constructed by conducting unrestrained membrane binding simulations of 10 ns duration, by placing the peptide molecules parallel to pre-equilibrated lipid bilayers at a distance of 2.5 nm, at an elevated temperature of 480 K to speed up insertion (using a simulation protocol from (18)). During the high-temperature insertion, hydrogen bonds in the helical peptides were restrained using distance restraints of 1000 kJ/(mol nm^2) to prevent unfolding. After cooling down to 303

K, a short equilibration run of 500 ps with position restraints of 1000 kJ/(mol nm^2) on the membrane-bound peptides was performed to allow temperature and volume to stabilize. Then, the systems were simulated for one microsecond in DMPC, and 700 ns in DMPC/DMPG, without any restraints at 303 K in the NPT ensemble, with snapshots saved every 50 ps. This unrestrained production simulation was conducted using a Nosé-Hover thermostat (19) and Parrinello-Rahman barostat at 1 bar (20) with semi-isotropic pressure coupling. A time step of 2 fs was used for all simulations, together with the LINCS algorithm (21) to constrain all bonds. Long-range electrostatics were treated via particle-mesh Ewald (22), combined with a 1.4 nm direct space cut-off for van der Waals and Coulomb interactions.

Peptide orientation. The orientation of the peptide was first determined independently by calculating τ and ρ directly from the simulation. From each simulation snapshot (taken every 50 ps) the τ and ρ angles were extracted and the average over all snapshots was calculated. The helix axis is defined for each snapshot as a vector pointing from the center of mass of the N-terminal half of the peptide to the center of mass of the C-terminal half of the peptide, taking into account only heavy backbone atoms in the helical part of the peptide, positions 3-16. The τ angle is calculated as the angle between this vector and the z-axis. The ρ angle is defined from an average position of the C_α-atoms for all residues in the helical part of the peptide, shifted to position 12 (by a shift of 100° per residue for an ideal α-helix). The error on ρ for each time step has been calculated as $\varepsilon_\rho(t) = \sqrt{1/(14 \cdot 13) \sum_{i=3}^{16} \left[\langle \rho(t) \rangle_{i \in [3;16]} - \rho_i(t)\right]^2}$.

To determine which initial part of the simulation should be discarded due to equilibration, an error analysis was performed, using the GROMACS tool *g_analyze.* The tool uses block averaging to estimate the error on the average of the time series of an observable, taking into account the correlation between chronologically close snapshots (23). The error was repeatedly calculated, while discarding different initial parts of the simulation between 10 and 200 ns. The final statistical analysis was done by discarding the initial interval which yielded the minimal sum of the errors for τ and ρ (see **Figure S2**). For DMPC the first 140 ns were discarded, and in the DMPC/DMPG simulation the first 160 ns were discarded.

Table S2. ^{2}H-NMR splittings (in kHz) back-calculated from the MD trajectory.

	DMPC			**DMPC/DMPG**		
Position	$\Delta\nu_q$	ε^a	**SD**[b]	$\Delta\nu_q$	ε^a	**SD**[b]
Gly-1	-11.8	2.5	35.3	-14.3	4.6	31.1
Ile-2	40.2	2.4	23.9	25.5	2.3	21.7
Gly-3	15.9	10.0	23.6	31.2	3.9	23.0
Lys-4	-7.3	3.2	23.3	-0.9	3.9	23.9
Phe-5	24.9	3.1	21.0	7.9	3.2	20.1
Leu-6	-30.8	2.4	13.2	-35.2	1.5	9.4
His-7	45.9	(12.3)	16.9	62.9	2.4	13.8
Ser-8	-34.8	0.7	9.2	-37.0	0.4	6.8
Ala-9	29.4	7.6	19.3	8.7	4.0	19.4
Leu-10	-15.9	9.0	18.0	-3.4	6.3	21.8
Leu-11	13.9	3.9	23.8	26.6	3.7	23.4
Phe-12	9.7	2.4	20.7	-7.0	3.5	20.7
Gly-13	-26.2	3.1	16.0	-33.0	2.0	11.7
Lys-14	31.5	11.7	21.8	56.9	5.0	19.5
Ala-15	-26.0	2.7	17.1	-28.6	2.9	15.9
Phe-16	33.5	(16.0)	20.7	25.6	4.9	21.3
Val-17	22.6	(43.8)	40.2	-31.8	3.6	14.1
Gly-18	-17.6	5.5	19.1	-7.9	6.5	25.0
Glu-19	-8.7	19.5	27.6	-24.9	(20.1)	19.2
Ile-20	38.6	(19.5)	27.6	50.5	5.8	25.7
Met-21	19.3	4.7	31.9	-6.3	11.8	33.7
Asn-22	-26.8	3.2	19.2	-25.2	10.2	18.6
Ser-23	-18.7	6.6	24.4	-1.6	8.2	35.6

[a] Error estimate from a block analysis using *g_analyze* (23). Brackets indicate that a fit was only possible by setting the fitting parameter τ_2 to either the total evaluated simulation length or to zero; i.e. insufficient statistics.

[b] Standard deviation of splittings over all snapshots of the simulation (discarding initial equilibration).

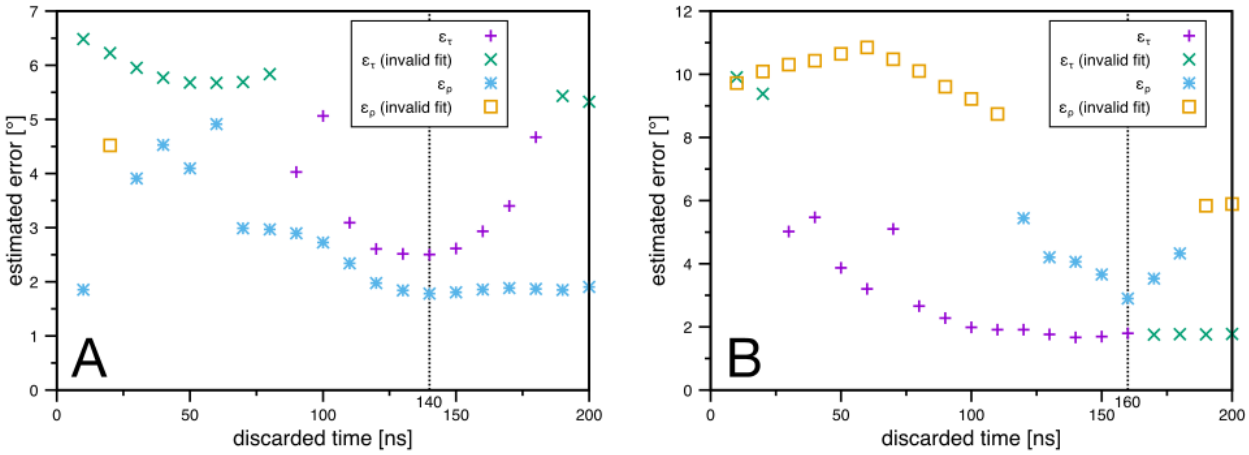

Figure S2. Estimated error for different discarded initial parts of the simulation, estimated with *g_analyze* (23). Data "invalid fit" indicate that a fit was only possible by setting the fitting parameter τ_2 to either the total evaluated simulation length or to zero; i.e. insufficient statistics. (A) MAG2 in DMPC, total simulation length 1 μs. The minimum of $\varepsilon_\tau + \varepsilon_\rho$ is at 140 ns. (B) MAG2 in DMPC/DMPG (3:1), total length 700 ns. The minimum of $\varepsilon_\tau + \varepsilon_\rho$ is at 160 ns.

The distributions of τ and ρ over the remaining part of the simulations (140-1000 ns in DMPC; and 160-700 ns in DMPC/DMPG (3:1)) were fitted to a Gaussian function to determine the standard deviations σ_τ and σ_ρ.

Hypothetical ^{2}H quadrupole splittings were then back-calculated from the orientation of the relevant C_α-C_β bonds of the native amino acids with respect to the membrane normal (the z-axis in the simulation box), which corresponds to the orientation of the external magnetic field in the NMR experiments. In the case of Gly residues, where no C_β atom is present, the corresponding C_α-H_α bond was used (i.e., as if the Gly residue was replaced by *L*-Ala). The quadrupole splittings were obtained from the simulations by calculating the bond order parameter $S_{CD}=½\langle 3\cos^2\theta - 1\rangle$, where θ is the angle between the C_α-C_β bond of the residue under consideration and the membrane normal, and multiplying this value with 84 kHz. The initial parts of the simulations, 140 ns for the DMPC system and 160 ns for DMPC/DMPG (3:1), were discarded to be consistent with the values for τ and ρ obtained directly, and the splittings were averaged over the rest of the simulation. The results are given in **Table S2**. The error on the splittings was calculated with *g_analyze* as mentioned above and as explained in (23).

To compare the NMR and MD results, the simulated ^{2}H-splittings were compared with the experimental ones, and the simulated ^{2}H-splittings were analyzed in the same way as the experimental splittings to determine the peptide orientation according to these splittings.

Peptide helicity. The helicity of the peptide in the simulations was determined for each residue based on the dihedral angles φ and ψ. If both of these angles are within 30° from the standard values for an α-helix, defined as φ = -57° and ψ = -47°, the residue is considered to be in a helical configuration, and the percentage helix is given by the number of time steps in which this condition is fulfilled, divided by the total number of time steps. This means that a residue is considered to be 100% helical if the condition is fulfilled for all evaluated time steps (140-1000 ns in DMPC, 160-700 ns in DMPC/DMPG).

Interaction analysis. The average position of the phosphorus atoms was calculated by averaging over the z-coordinate of the phosphorus of all lipids in the upper leaflet, but discarding snapshots where the peptide's center of mass was closer than 2 nm to the phosphorus atom, to ignore the influence of the peptide on the position of the lipid head groups. The error on the average was obtained by calculating average values for each lipid and then calculating the statistical error from these averages:

$$\varepsilon_{Pz} = \sqrt{1/(N(N-1))\sum_{i=1}^{N}\left[\langle P_{z,all}\rangle - \langle P_{z,i}\rangle\right]^2}.$$

The error on the z-coordinate of the oxygens of Glu-19, Ser-23 and MAG2 was estimated using *g_analyze*. The values and errors are given in **Table S3**. The average membrane center was determined by averaging the values obtained for the undisturbed phosphorus of the upper leaflet and all phosphorus of the lower leaflet.

Table S3. Average z coordinates with respect to the membrane center. Brackets indicate that a fit was only possible by setting the fitting parameter τ_2 to either the total evaluated simulation length or to zero; i.e. insufficient statistics.

	Δz to membrane center (nm)	Error (nm)
DMPC		
P upper leaflet, excluding lipids within 2 nm of peptide	1.70	0.01
MAG2 (center of mass)	1.20	0.09
Glu-19, O1	1.71	(0.22)
Glu-19, O2	1.71	(0.22)
Ser-23, O1	1.92	(0.17)
Ser-23, O2	1.92	(0.16)
DMPC/DMPG (3:1)		
P upper leaflet, excluding lipids within 2 nm of peptide	1.79	0.01
MAG2 (center of mass)	1.06	
Glu-19, O1	1.46	0.05
Glu-19, O2	1.48	(0.04)
Ser-23, O1	1.82	0.07
Ser-23, O2	1.81	0.07

^{2}H-NMR SPLITTINGS

The splittings were determined from the NMR spectra. In all cases a central peak was observed, which is due in part to residual ^{2}H nuclei in water and can be observed also in samples without peptide. The ^{2}H-NMR signals from peptides in the oriented membranes give two symmetrical peaks with a splitting dependent on the orientation of the C-CD_3 bond. Spectra are shown in **Figure 2** in the main text, but are also included here in **Figures S3 and S4** enlarged and scaled to better show the signals and indicate the splittings.

In POPC/POPG samples, splittings are usually clearly visible. They are shown in red in **Figure S3A**. In MAG-F12A no splitting is seen, probably because it happens to be too small to be resolved form the central peak. It is assumed that the splitting in this case is 0 kHz. This value fits the helical curve obtained from a fit to the other data points, supporting this interpretation (**Figure 4C**). There are some additional splittings with low intensity visible in the spectra (marked in blue). In MAG2-F12A, there is a shoulder on the main peak, with a possible splitting of around 8 kHz, but the intensity is very low. In MAG2-V17A, a splitting of approximately 38 kHz is seen. This is a value typically found for aggregated peptides (24), and can therefore be due to some immobilized peptide fraction. In MAG2-I20A there is a smaller splitting seen, 14.1 kHz, which is very close to half the main splitting. This is most likely a signal from peptides in unoriented vesicles, where fast rotation around the bilayer normal will give a splitting averaged by a factor of ½ (7).

In DMPC/DMPG at P/L=1:100, clear splittings are seen in all cases, marked in red in **Figure S3B**. In MAG2-F5A there is also a smaller intensity splitting (marked in blue), which equals half the main splitting, most likely also due to unoriented parts of the sample.

In DMPC/DMPG at P/L=1:50 (**Figure S4A**), splittings are harder to define. In MAG2-F5A, -F12A, and -G18A, only a central peak is found. In the other cases, splittings are seen (marked in red), but are sometimes not as clear as in DMPC/DMPG at P/L=1:100. Even though the amount of peptide per sample is the same in both cases, the intensity of the ^{2}H-NMR signal from the peptide is lower at the higher concentration for some unknown reason. It could have something to do with a change in mobility which can affect relaxation behavior. In MAG2-V17A, there are two possible splittings with similar intensities. The smaller splitting is 29.9 kHz. The larger splitting (marked in blue) is 36.8 kHz, close to the powder splitting, and therefore somewhat suspicious since it could be due to immobilized peptides. In MAG2-I20A there are

also two possible splittings. The smaller one (7.9 kHz) has a higher intensity, which might be because it is close to the central peak and overlaps with the flanks of the central peak. The larger one (13.5 kHz) is slightly asymmetric around the central peak. Since also here the smaller splitting is close to ½ of the larger one, it may be due to signals from unoriented parts of the sample (like for MAG2-F5A in DMPC/DMPG P/L=1:50). We can note that the clearest splittings (from MAG2-L6A, -A9, -G13A, -A15 and -F16A) are not very different from the splittings at the same position in DMPC/DMPG P/L=1:100 (within 5 kHz). This indicates that the peptide orientation is not changing much, and makes it likely that also the other splittings should be quite similar. This would make it more likely that the splitting of MAG2-V17A is 29.9 kHz rather than the larger splitting of 36.8 kHz also seen, and that the splitting of MAG2-I20A is 13.5 kHz rather than 7.9 kHz. The similarity of splittings at 1:100 and 1:50 also makes it reasonable to assume that the splitting of MAG2-F12A can be close to 0 kHz, but this assumption cannot be made for MAG2-F5A and MAG2-G18A, where large splittings were observed in DMPC/DMPG P/L=1:100. Therefore the spectra of MAG2-F5A and MAG2-G18A are not assigned a splitting and are not included in the analysis.

Several fits were made using different combinations of data in DMPC/DMPG P/L=1:50, as shown in **Figure S5** and **Table S4**. For position 18, 29.9 kHz or 36.8 kHz were used, and for position 20, either 13.5 kHz or 7.9 kHz. In all cases, a very similar best fit was found, within 1° of the fit shown in the main text, with tau = 94° and rho = 174° (**Figure S3, A-C**). Also when positions 18, 20, or both were not used at all in the fit, the same result was found (**Figure S3, D-F**), so the exact splittings of these positions were not critical for the result.

Finally, in DMPC/DMPG (**Figure S4B**) with PGLa, no clear splittings are seen in MAG2-F5A, -A9 and -F12A. In the other samples, clear splittings are seen (marked in red). These splittings are sometimes very different from the splittings found in DMPC/DMPG without PGLa (up to 30 kHz changes in the absolute values), and therefore it is not possible to assume anything about the spectra without clear splittings. It is possible that those splittings are really zero, but it could also be a problem with signal intensities. Therefore those positions were not assigned a splitting and are not used in the data analysis.

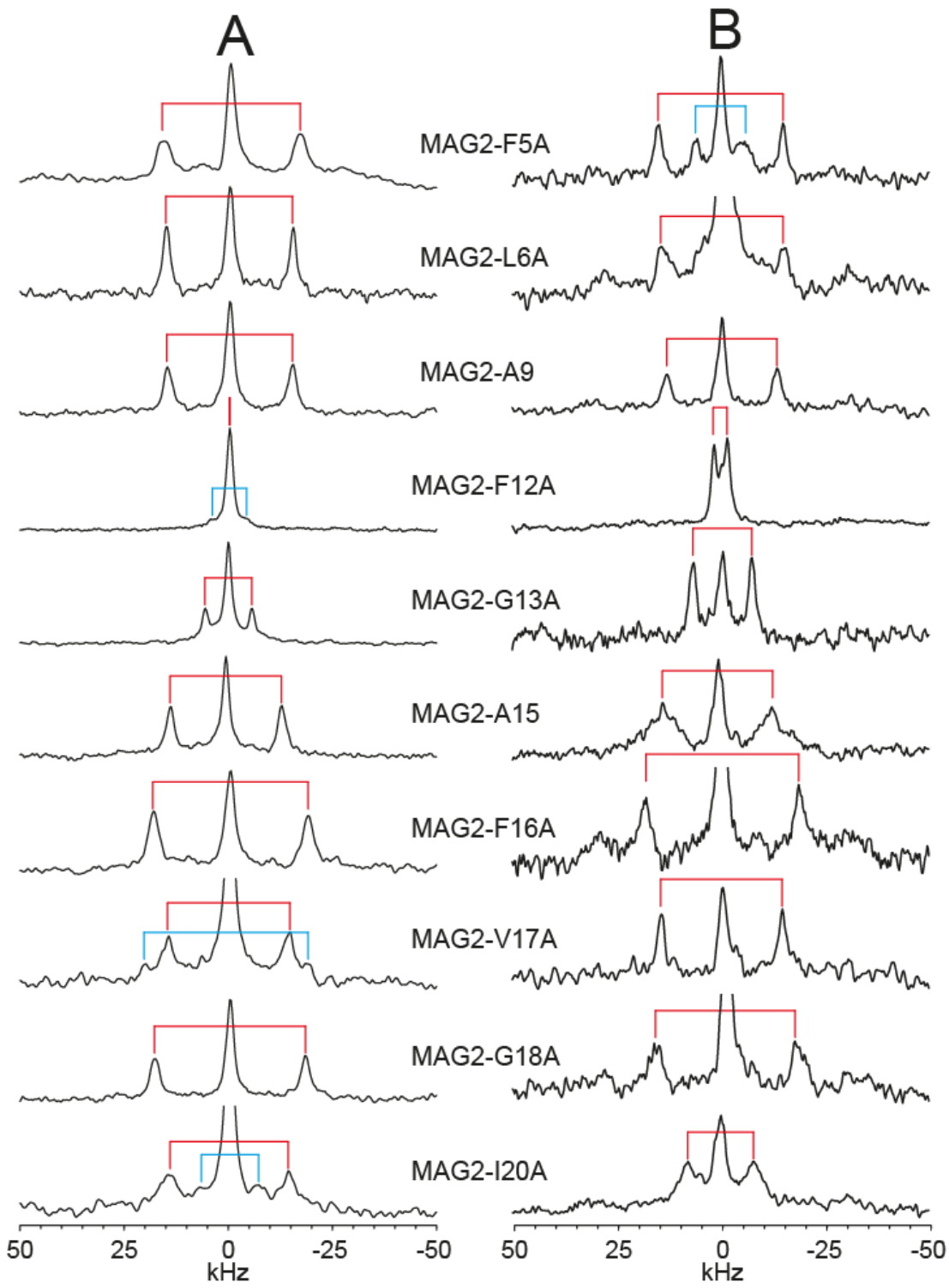

Figure S3. Splittings found in ^{2}H-NMR spectra. (A) MAG2 in POPC/POPG (9:1). (B) MAG2 in DMPC/DMPG (3:1), P/L=1:100. Main splittings are marked in red, minor splittings in blue. All samples were prepared using method 1.

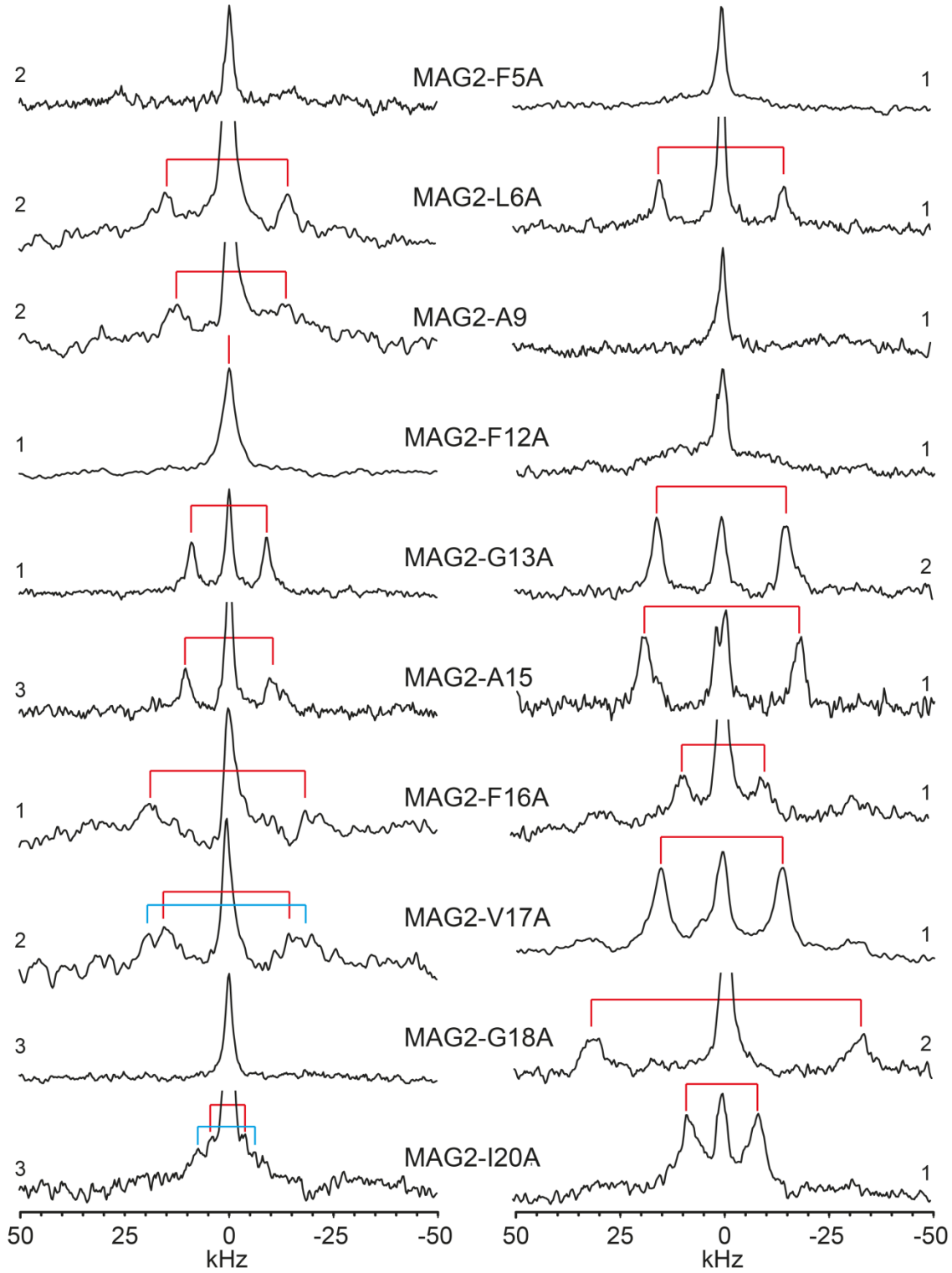

Figure S4. Splittings found in ^{2}H-NMR spectra. (A) MAG2 in DMPC/DMPG (3:1). P/L=1:50. (B) MAG2 with PGLa in DMPC/DMPG (3:1), P/P/L=1:1:100. Main splittings are marked in red, minor splittings in blue. Numbers next to each spectrum indicate the sample preparation method used.

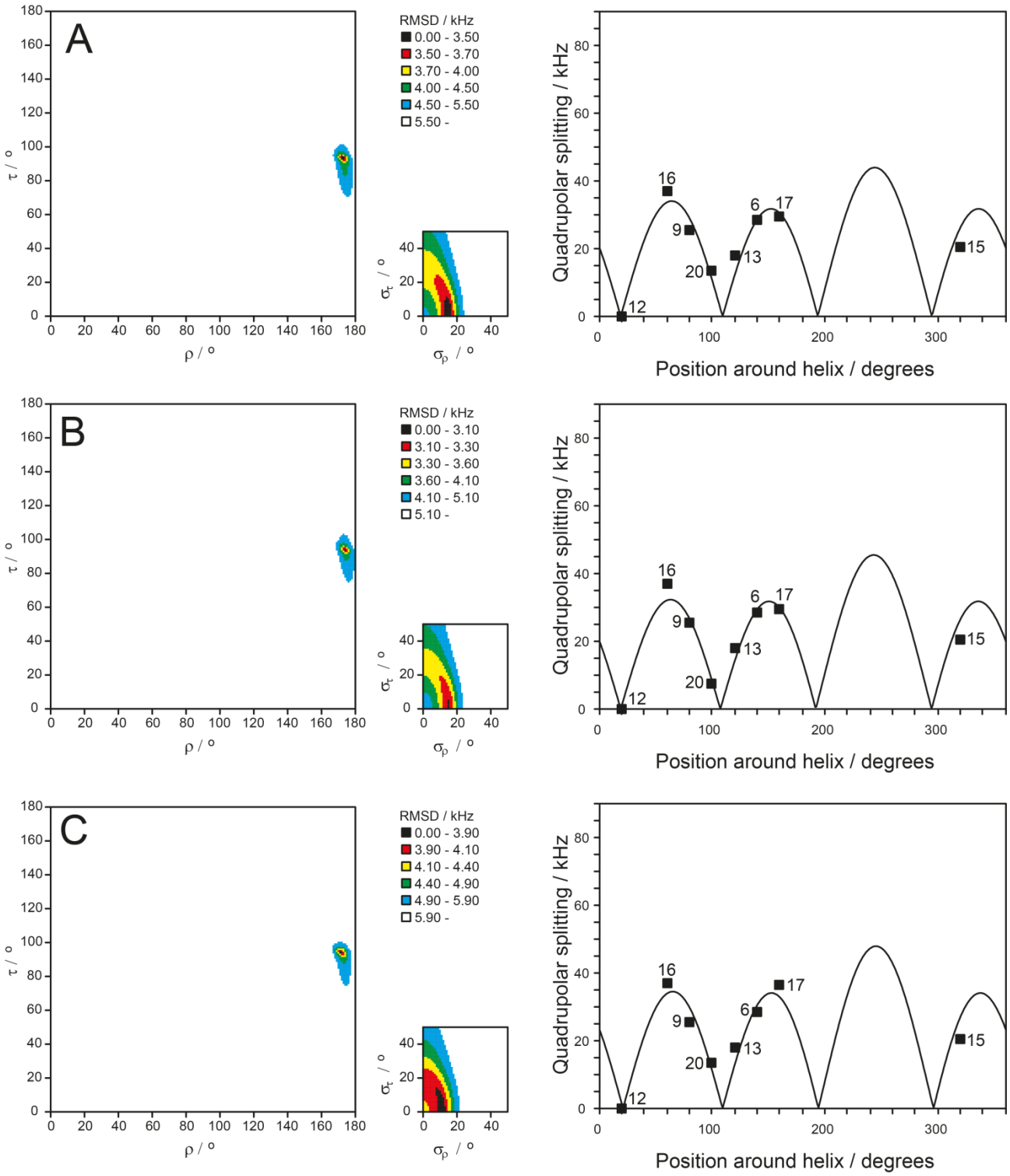

Figure S5. Fits of various data sets for MAG2 in DMPC/DMPG (3:1). P/L=1:50. (A) Fit using values from Table 1 in the main text. (B) Like (A), but using for position 20 a splitting of 7.9 kHz. (C) Like (A), but using for position 17 a splitting of 36.8 kHz.

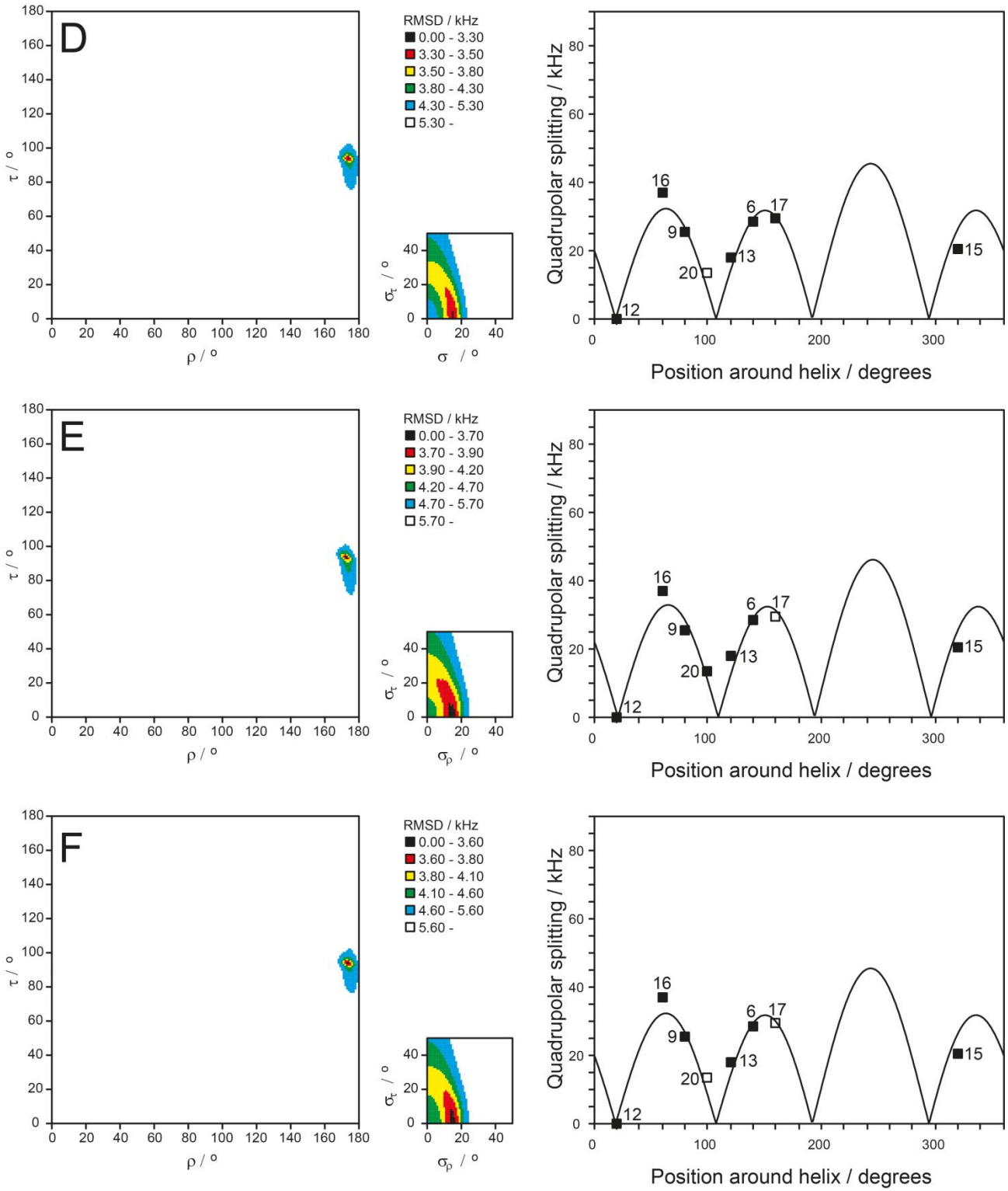

Figure S5 (continued). Fits of various data sets for MAG2 in DMPC/DMPG (3:1). P/L=1:50. (D) Fit not using data from position 20. (E) Fit not using data from position 18. (F) Fit not using data from position 18 and 20.

Table S4. Fits of MAG2 in DMPC/DMPG P/L=1:50, using different ^{2}H-NMR data sets.

Method	Lipid system	P/L	Positions used in fit	τ (°)	ρ (°)	σ_τ (°)	σ_ρ (°)	RMSD (kHz)
^{2}H-NMR	DMPC/DMPG	2:75:25	8 [a]	93	173	1	15	3.4
	DMPC/DMPG	2:75:25	8 [b]	94	174	1	15	3.1
	DMPC/DMPG	2:75:25	8 [c]	94	172	0	11	3.8
	DMPC/DMPG	2:75:25	7 [d]	94	174	1	15	3.3
	DMPC/DMPG	2:75:25	7 [e]	94	174	1	15	3.3
	DMPC/DMPG	2:75:25	6 [f]	94	174	1	15	3.5

[a] 5, 18 not used. 17 = 29.9 kHz, 20 = 13.5 kHz.

[b] 5, 18 not used. 17 = 29.9 kHz, 20 = 7.6 kHz.

[c] 5, 18 not used. 17 = 36.8 kHz, 20 = 13.5 kHz.

[d] 5, 17, 20 not used.

[e] 5, 17, 18 not used.

[f] 5, 17, 18, 20 not used.

HELICAL WHEELS OF MAGAININ 2 AND PGLA IN MEMBRANES

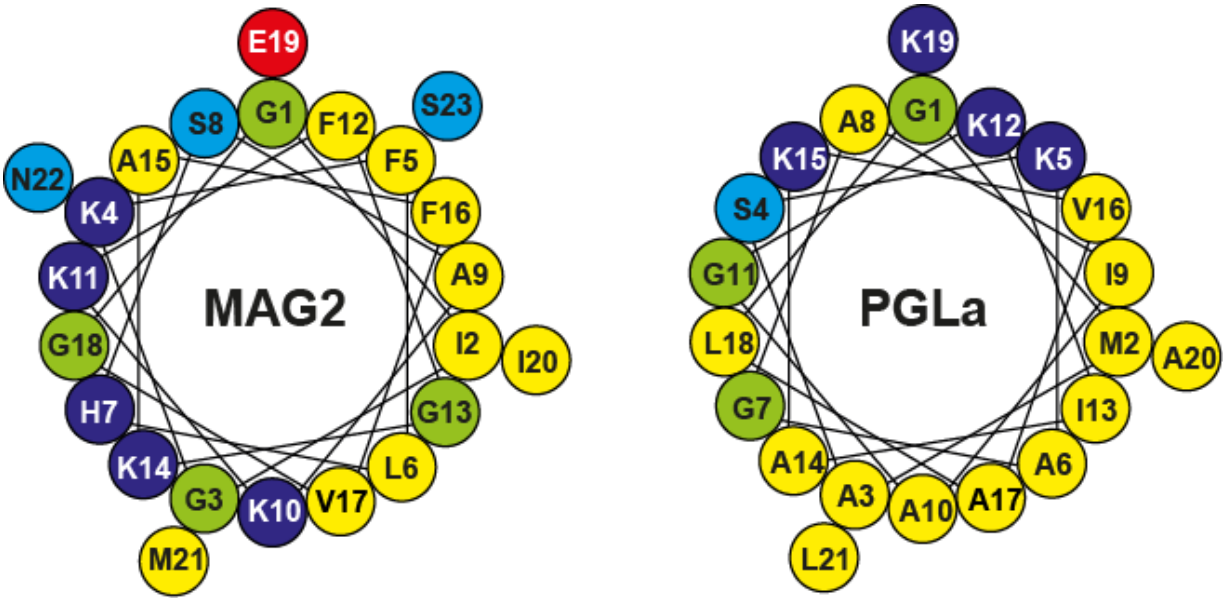

Figure S6. Helical wheels of MAG2 and PGLa. Hydrophobic residues are marked in yellow, polar in light blue, cationic in dark blue, anionic in red, glycines in green.

ORIENTATION OF MAGAININ 2 IN MEMBRANES

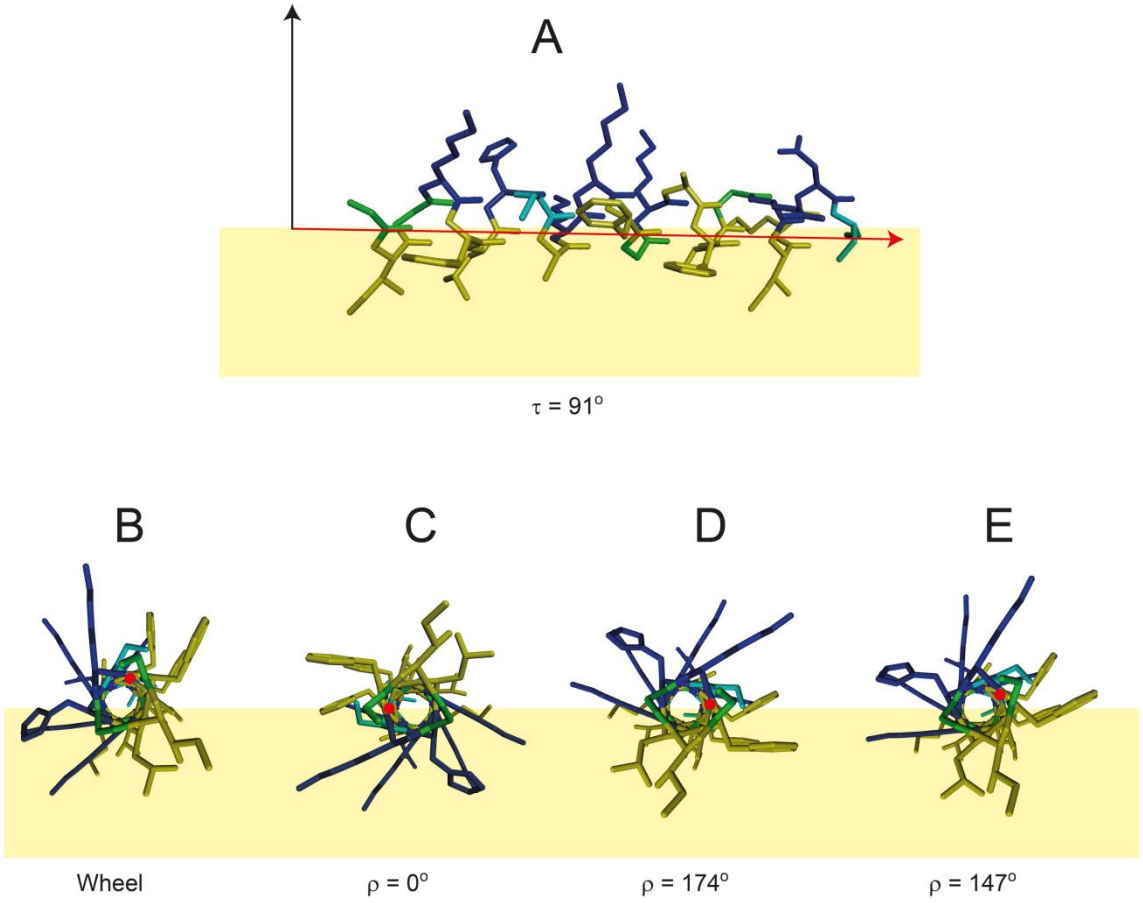

Figure S7. Illustration of the orientation of MAG2 in membranes according to a fit of ^{2}H-NMR data. The peptide is seen along the axis in a stick representation, where hydrophobic residues are yellow, Lys and His dark blue, Glu light blue and Gly green. The hydrophobic part of the membrane is shown as a yellow box (thickness not in scale). (A) MAG2 seen from the side in the membrane. The tilt angle (τ) of 91° means that the helix axis (red arrow), from N- to C-terminal, is rotated 91° from the membrane normal (black arrow). The C-terminus is inserted slightly deeper into the membrane than the N-terminus. (B-E) MAG2 seen along the helix axis, with the C-terminus in front, flat on the membrane. The red dot shows the position of C_α of the reference residue Phe-12. (B) Orientation as in the helical wheel in **Figure S6**. C_α of position 1 points up. (C) Reference orientation where the azimuthal angle ρ is set to 0°. In this case, a vector from the helix axis to C_α of Phe-12 lies in the plane of the membrane. (D) The orientation found for MAG2 alone in POPC/POPG or DMPC/DMPG lipids, with ρ = 174°. All charged residues point out of the membrane. (E) The orientation found for MAG2 together with PGLa in DMPC/DMPG lipids, with ρ = 147°. In this case, C_α of Lys-10 is deeper in the membrane, and C_α of Glu-21 is pointing more to the water. The charged residues can snorkel so that the charges are outside the membrane even if C_α is deeper down. It should also be noted that the depth of membrane insertion is not known from the NMR data, here in all cases the helix axis is shown to be in the plane of the membrane.

SUPPORTING REFERENCES

1. Fields, G. B., and R. L. Noble. 1990. Solid-phase peptide synthesis utilizing 9-fluorenylmethoxycarbonyl amino acids, *Int. J. Pept. Protein Res.* 35:161-214.
2. Strandberg, E., J. Zerweck, D. Horn, G. Pritz, P. Wadhwani, M. Berditsch, J. Bürck, and A. S. Ulrich. 2015. Influence of hydrophobic residues on the activity of the antimicrobial peptide magainin 2 and its synergy with PGLa, *J. Pept. Sci.* 21:436-445.
3. Rance, M., and R. A. Byrd. 1983. Obtaining high-fidelity spin-1/2 powder spectra in anisotropic media - phase-cycled Hahn echo spectroscopy, *J. Magn. Reson.* 52:221-240.
4. Davis, J. H., K. R. Jeffrey, M. Bloom, M. I. Valic, and T. P. Higgs. 1976. Quadrupolar echo deuteron magnetic resonance spectroscopy in ordered hydrocarbon chains, *Chem. Phys. Lett.* 42:390-394.
5. Strandberg, E., N. Kanithasen, J. Bürck, P. Wadhwani, D. Tiltak, O. Zwernemann, and A. S. Ulrich. 2008. Solid state NMR analysis comparing the designer-made antibiotic MSI-103 with its parent peptide PGLa in lipid bilayers, *Biochemistry*. 47:2601-2616.
6. Glaser, R. W., C. Sachse, U. H. N. Dürr, S. Afonin, P. Wadhwani, E. Strandberg, and A. S. Ulrich. 2005. Concentration-dependent realignment of the antimicrobial peptide PGLa in lipid membranes observed by solid-state ^{19}F-NMR, *Biophys. J.* 88:3392-3397.
7. Strandberg, E., S. Özdirekcan, D. T. S. Rijkers, P. C. A. Van der Wel, R. E. Koeppe, II, R. M. J. Liskamp, and J. A. Killian. 2004. Tilt angles of transmembrane model peptides in oriented and non-oriented lipid bilayers as determined by ^{2}H solid state NMR, *Biophys. J.* 86:3709-3721.
8. Strandberg, E., P. Wadhwani, P. Tremouilhac, U. H. N. Dürr, and A. S. Ulrich. 2006. Solid-state NMR analysis of the PGLa peptide orientation in DMPC bilayers: structural fidelity of ^{2}H-labels versus high sensitivity of ^{19}F-NMR, *Biophys. J.* 90:1676-1686.
9. Davis, J. H. 1983. The description of membrane lipid conformation, order and dynamics by ^{2}H-NMR, *Biochim. Biophys. Acta*. 737:117-171.
10. Glaser, R. W., C. Sachse, U. H. N. Dürr, P. Wadhwani, and A. S. Ulrich. 2004. Orientation of the antimicrobial peptide PGLa in lipid membranes determined from ^{19}F-NMR dipolar couplings of 4-CF_3-phenylglycine labels, *J. Magn. Reson.* 168:153-163.
11. Strandberg, E., S. Esteban-Martín, J. Salgado, and A. S. Ulrich. 2009. Orientation and dynamics of peptides in membranes calculated from ^{2}H-NMR data, *Biophys. J.* 96:3223-3232.
12. Strandberg, E., and A. S. Ulrich. 2014 Dynamic structure analysis of peptides in membranes by solid-state NMR, *In* Advances in Biological Solid-State NMR: Proteins and Membrane-Active Peptides. F. Separovic, and A. Naito, editors. Royal Society of Chemistry, London, pp. 304-319.
13. Jorgensen, W. L., J. Chandrasekhar, J. D. Madura, R. W. Impey, and M. L. Klein. 1983. Comparison of simple potential functions for simulating liquid water, *J. Chem. Phys.* 79:926-935.
14. Jämbeck, J. P., and A. P. Lyubartsev. 2012. Derivation and systematic validation of a refined all-atom force field for phosphatidylcholine lipids, *J. Phys. Chem. B.* 116:3164-3179.
15. Lindorff-Larsen, K., S. Piana, K. Palmo, P. Maragakis, J. L. Klepeis, R. O. Dror, and D. E. Shaw. 2010. Improved side-chain torsion potentials for the Amber ff99SB protein force field, *Proteins*. 78:1950-1958.

16. Reißer, S. 2014. Computational studies of membrane-active antimicrobial peptides and comparison with NMR data. PhD thesis. Karlsruhe Institute of Technology, Karlsruhe.
17. Case, D. A., T. A. Darden, …, P. A. Kollman 2012 *AMBER 12*, University of California, San Francisco.
18. Ulmschneider, J. P., J. C. Smith, M. B. Ulmschneider, A. S. Ulrich, and E. Strandberg. 2012. Reorientation and dimerization of the membrane-bound antimicrobial peptide PGLa from microsecond all-atom MD simulations, *Biophys. J.* 103:472-482.
19. Nosé, S. 1984. A molecular dynamics method for simulations in the canonical ensemble, *Mol. Phys.* 52:255-268.
20. Parrinello, M., and A. Rahman. 1981. Polymorphic transitions in single crystals - a new molecular dynamics method, *J. Appl. Phys.* 52:7182-7190.
21. Hess, B., H. Bekker, H. J. C. Berendsen, and J. G. E. M. Fraaije. 1997. LINCS: A linear constraint solver for molecular simulations, *J. Comp. Chem.* 18:1463-1472.
22. Darden, T., D. York, and L. Pedersen. 1993. Particle mesh Ewald - an $N \bullet \log(N)$ method for Ewald sums in large systems, *J. Chem. Phys.* 98:10089-10092.
23. Hess, B. 2002. Determining the shear viscosity of model liquids from molecular dynamics simulations, *J. Chem. Phys.* 116:209-217.
24. Strandberg, E., D. Tiltak, S. Ehni, P. Wadhwani, and A. S. Ulrich. 2012. Lipid shape is a key factor for membrane interactions of amphipathic helical peptides, *Biochim. Biophys. Acta*. 1818:1764-1776.